ELSEVIER

Journal of Power Sources 52 (1994) 17–24

JOURNAL OF POWER SOURCES

The effect of alloying with antimony on the electrochemical properties of lead

R. Babić[a], M. Metikoš-Huković[a], N. Lajqy[a], S. Brinić[b]

[a]Department of Electrochemistry, Faculty of Chemical Engineering and Technology, University of Zagreb, Savska 16, 41000 Zagreb, Croatia

[b]Faculty of Technology, University of Split, N Tesle 10, 58000 Split, Croatia

Received 1 February 1994; accepted 17 March 1994

Abstract

The electrochemical behaviour of lead, antimony and lead–antimony binary alloys has been studied as a function of sulfuric acid and antimony concentrations in the lead alloy. The investigation was performed by means of cyclic voltammetry and impedance spectroscopy methods. Cyclic voltammetry, performed between the hydrogen and oxygen evolution and over narrower regions of potential coupled with systematic variation of the scan rates and the positive or negative reversal potential, revealed more details on the oxidation and reduction processes in the potential region of Pb(II)-, Pb(IV)- and Sb(III)-containing species which give further insight into the nature of the reactions of the lead/acid battery. The impedance measurements performed in the potential range of lead oxide, in which antimony oxidation in the alloys takes place, show the decrease in film resistance with increasing antimony content.

Keywords: Lead alloys; Antimony; Lead/acid batteries

1. Introduction

When a lead electrode is polarized in sulfuric acid solution in the potential range between hydrogen and oxygen evolution, a number of electrochemical reactions have been observed and studied. For example, Pavlov and co-workers [1–4] have studied the mechanism of the electrochemical oxidation and the crystal structure of the Pb electrode, while others investigated the analysis of each redox process occurring on the Pb electrode [5–22]. The two reactions taking place at the $Pb/PbSO_4$ and $PbO_2/PbSO_4$ reversible potentials correspond to the charge and discharge reactions of the negative and positive electrodes in the lead/acid battery. Within the range of these two potentials the formation of several lead compounds occurs, forming a dense crystalline layer, and passivates the Pb electrode. The layer composition depends on the potential and the quantity of electricity passed, as well as the alloying elements in the lead substrate.

Antimony is widely used as an alloying additive in Pb alloys for the casting of lead/acid battery grids. It has been established that Sb affects significantly not only the casting and the mechanical properties of the alloys but also has a strong impact on the electrochemical processes of the positive plate of the battery. Therefore, the electrochemical behaviour of Sb [23–30], as well as the influence of Sb on the electrochemical behaviour of Pb in Pb–Sb alloys [5,8,11,12,16,31–42] has been extensively studied during the last few years. In spite of that, the influence of Sb on electrochemical behaviour of Pb is not yet unambiguously explained and some contradictory results still exist in the literature. This is not surprising since the system is complex, and many factors influence its electrochemical behaviour. The aim of the present work was to study the electrochemical behaviour of Pb–1.3 to 4.5 wt.% Sb alloys and to compare the results obtained with the electrochemical behaviour of pure metals.

2. Experimental

The investigation was performed on pure Pb (99.998 wt.%), spectroscopically clean Sb (Johnson Matthey Co.) and Pb–Sb alloys with a content of 1.3, 2.75, 3.75 and 4.5 wt.% Sb by means of cyclic voltammetry (CV) and electrochemical impedance spectroscopy (EIS). The structure and morphology of Pb and Pb alloys were analysed by means of scanning electron microscope (SEM). The electrodes had a cylindrical form. The lateral surface of the cylinder was insulated by Araldite,

SSDI 0378-7753(94)01925-L

exposing only the cylinder base plane to the solution (the surface area of Sb was 0.46 cm^2 and that of Pb and Pb alloys 0.283 cm^2). Before each experiment the Pb and Pb-alloy electrodes were polished with the silicon carbide grinding paper (grit 600), degreased in triclorethylene, rinsed with distilled water and prior to each measurement polarized for 10 min at −1.0 V, below the equilibrium potential of the $Pb/PbSO_4$ couple, to remove oxide formed on the surface due to contact with air and $PbSO_4$ formed during the immersion. Before the measurements, the Sb electrode was polished mechanically, wiped with tissue paper, and dipped in ethanol to remove dust and grease from the surface. Mechanical polishing was used giving reproducible results. Most measurements were started after a short stand (5 to 10 min) at the rest potential to clean the electrode surface from oxidation products. In fact, the potential measured is a mixed potential determined by the reactions of anodic oxidation of Sb and cathodic reduction of oxygen [23].

The aqueous 5, 0.5 and 0.05 M H_2SO_4 solutions were used as electrolytes. Electrochemical measurements on pure Sb were performed in sulfuric acid solution saturated with Sb_2O_3 in order to prevent big changes in the concentration of Sb in solution due to its dissolution. The experiments were performed in a standard two-compartment glass cell at 298 K. The counter electrode was a large platinum plate, and the reference electrode was a saturated calomel electrode (SCE). All potential values in the paper are presented versus the SCE.

The CV measurements were performed with a potentiostat (Wenking, PCA 72H), a voltage scan generator (Wenking, VSG 72), and a recorder (Servogor Goerz, XY 773).

The EIS measurements were performed with an EG&G Princeton applied research model 273 potentiostat, and EG&G model 5315 lock-in amplifier controlled by an IBM PC computer.

3. Results and discussion

3.1. Cyclic voltammetry on pure lead

The typical curve of cyclic voltammogram for the Pb electrode in a 5 M sulfuric acid solution obtained by sweeping the potential in a region from the potential of the hydrogen evolution to the potential of the oxygen evolution and reversing it cathodically to the starting potential is shown in Fig. 1. The potential sweep of a pure-Pb electrode in the positive direction first shows peak A_1 corresponding to the formation of $PbSO_4$ layer. Its formation proceeds via both a solid-state reaction and a precipitation from a soluble Pb(II) species produced by oxidation of the Pb electrode [43].

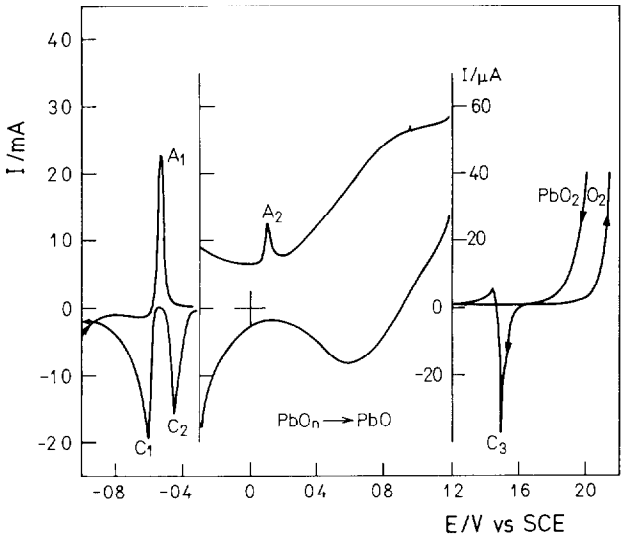

Fig. 1 Cyclic voltammogram on a Pb electrode in a 5 M H_2SO_4 solution, sweep rate 10 mV s^{-1}

It has been pointed out by Pavlov [44,45] and Ruetschi [31] that the $PbSO_4$ film on Pb acts as a perm-selective membrane which becomes impermeable to SO_4^{2-} and HSO_4^- when it has reached a thickness of 1 to several μm. Only migration and diffusion of the H^+ or OH^- ions through the $PbSO_4$ intercrystalline spaces can occur to carry the current. Therefore, underneath the $PbSO_4$ membrane, the pH increases and tetragonal lead monoxide (tetra-PbO) and basic lead sulfates are formed. In the linear sweep voltammetry experiments, the oxidation peak of Pb to PbO can be hardly noticed on voltammetric curves. Only when more sensitive measurements of the current in the anodic passivated region are made, small anodic current peak A_2 can be observed, as it is shown in Fig. 1.

At potentials above 1.0 V, the PbO of the corrosion layer is oxidized to non-stoichiometric PbO_n ($1<n<2$) which behaves as a semiconductor [3,15,16]. When the potential increases, n increases too and when the former reaches a critical value, α-PbO_2 nucleation will start. The crystal lattices of tetra-PbO and α-PbO_2 are quite similar and therefore α-PbO_2 formation can be realized in the bulk of the oxide under the action of the O atoms and $O^{\cdot}$ radicals which are products of the oxygen evolution [46]. α-PbO_2 is stable in alkaline solutions and therefore can be formed underneath the $PbSO_4$ perm-selective membrane. The other modification, β-PbO_2 is stable in acid solutions and therefore its formation occurs by $PbSO_4$ oxidation at the $PbSO_4/H_2SO_4$ interface. Both α- and β-PbO_2 formation proceeds by a nucleation growth mechanism [15, 47].

Fig. 1 shows that no current maximum for the formation of any PbO_2 modification can be observed on the potential–current curve near the $PbSO_4/PbO_2$ potential. The increase in anodic current above about 1.8 V signifies both the oxidation of $PbSO_4$ to β-PbO_2 and

the evolution of oxygen. The current peaks corresponding to α- and β-PbO_2 formation can be only observed by cycling sweeping in a potential region between 0 V and the potential of oxygen evolution, as was reported by several authors [11,15,19]. It can be seen that the oxygen-evolution current exhibits large positive hysteresis, i.e., current recorded on the backward (negative-going) scan is much greater than those recorded on the forward (positive-going) scan at potentials above 1.7 V. This phenomenon can be explained in terms of the large nucleation overpotential required to initiate the growth of β-PbO_2 nuclei in the compact polycrystalline layer of $PbSO_4$ formed earlier in the forward scan. Since it is known that oxygen evolution proceeds on β-PbO_2 [47] it can be assumed that on the forward scan there is always a delay in the appearance of the oxygen-evolution current until sufficient β-PbO_2 has nucleated and grown in the $PbSO_4$ layer. On the backward scan the nucleation of β-PbO_2 is of less importance because sufficient β-PbO_2 already exists and, hence, the oxygen-evolution current persists at a high level when the direction of the linear potential scan is reversed.

Reversing the direction of potential sweep it can be seen that, during its early part, a complex mixture of anodic and cathodic activities can be observed. The complexity of voltammetric peaks are caused by simultaneous cathodic and anodic reactions that occur in this potential range. These are the PbO_2 discharge (peak C_3) and the oxidation of the lead substrate and/or some incompletely oxidized products of Pb, because an anodic current is not observed when PbO_2 is reduced on an inert substrate [17,48]. In the literature, the oxidation product has been suggested to be divalent [7,8], trivalent [9] as well as tetravalent lead [5]. According to Sharpe [7,8] the structure of the anodic current is caused by an overlap of the reduction currents of both polymorphs α-PbO_2 and β-PbO_2. β-PbO_2 is reduced at higher and α-PbO_2 at lower potentials of peak C_3.

As a result of the reduction of PbO_2, the corrosion layer becomes thinner or is partially destroyed, and the anodic reaction of lead oxidation is accelerated at these places. The $PbSO_4$ layer is forming on the surface of the discharging PbO_2. Due to its perm-selectivity the pH increases underneath it and the conditions for the lead oxide formation are fulfilled. As a consequence the rate of the reaction of lead oxidation decreases. Parallel to this process, there is a reduction of the non-stoichiometric lead oxide, PbO_n $(1<n<2)$ [32]. The reaction becomes dominating below 0.9 V in 5 M H_2SO_4 and the current becomes cathodic.

When the potential reaches a value of -0.47 V, the cathodic peak C_2 appears. The potential and the current of peak C_2 depend on the polarization time, on the potential value at which the electrode was prepolarized anodically and on the sulfuric acid concentration. The longer the time of anodic polarization, the more negative the potential of peak C_2 is and the higher the peak becomes [20]. The height of peak C_2 significantly increases with the increase of acid concentration (see section 3.3). It is widely accepted [13–15,20,21,44] that peak C_2 corresponds to the reduction of tetra-PbO. Recently Guo [22] has confirmed this by laser Raman scattering and X-ray diffraction. During the anodic oxidation of the lead electrode, a small amount of basic lead sulfate is formed in the $PbSO_4$ intercrystalline spaces [49,50] prior to that of tetra-PbO. Its amount is so small that the reduction peak cannot appear in the common linear potential sweep.

At potentials lower than about -0.55 V, reduction of $PbSO_4$ occurs, which is reflected in the cathodic peak C_1.

3.2. Cyclic voltammetry on pure antimony

From the previous paragraph it can be seen that the processes occurring during the polarization of Pb in sulfuric acid solutions have been well elucidated. It is not, however, the case with Sb, which electrochemical behaviour in sulfuric acid solutions has been systematically investigated during the last few years [23–30].

Cyclic voltammogram of an Sb electrode measured in the potential range from -0.8 to $+0.3$ V in a 0.05 M H_2SO_4 solution saturated with Sb_2O_3 is shown in Fig. 2.

When Sb dissolves anodically it can be expected that when the concentration of Sb ions, close to the electrode surface, exceeds a certain value formation of a surface film will start leading to passivation of the electrode. Fig. 2 confirms this statement. The active dissolution of Sb ends with the first current maximum, A', which is probably due to the formation of a surface film which starts to passivate the electrode. Inasmuch as the formation of antimony(V) species in sulfuric acid solution was not observed, even at higher potentials [26,30], the

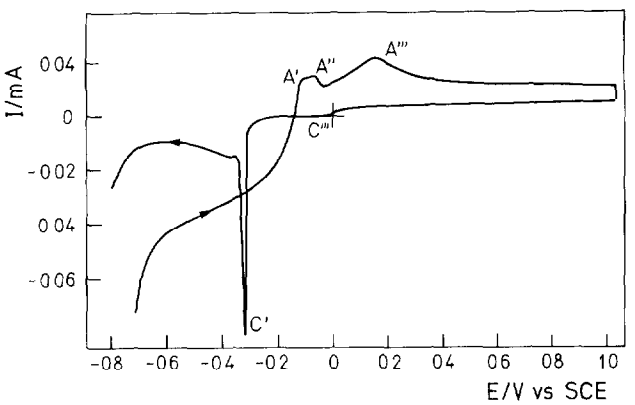

Fig 2. Cyclic voltammogram on an Sb electrode in a 0.05 M H_2SO_4 solution saturated with Sb_2O_3; sweep rate 1 mV s^{-1}.

other two current peaks, A″ and A‴, can only correspond to phase transitions in the Sb(III) oxide/hydroxide surface layer. During the cathodic sweep a cathodic arrest C‴ and well-expressed current peak C′ at −0.32 V can be observed. However, if the direction of the cathodic sweep is reversed just after the third anodic current peak, two cathodic current arrests could be observed before the current peak C′.

Pavlov et al. [24] assumed that the anodic layer was built of amorphous SbOOH which forms a gel-like film containing water. The amorphous SbOOH layer interacts with sulfuric acid solution and is dissolved as SbO^+ ions or some Sb(III)-hydrated species depending on the acid solution [29]. The amorphous, gel-like oxide/hydroxide anodic layer only partly passivates the electrode and the dissolution of trivalent Sb continuous depending on the acid concentration [25].

After the third peak, the current decreases gradually and reaches finally a constant value (Fig. 2); the electrode surface becomes completely passivated. No oxygen evolution can be visually observed and no further current peaks appear. Thus, it can be concluded that the electronic conductivity is strongly inhibited at this electrode. Since SbOOH is a thermodynamically unstable species, it undergoes dehydration, as scanning proceeds to more positive potentials, leading to Sb_2O_3. The multiple anodic peaks can be interpreted as the nucleation and spreading of successive hydroxide/oxide layers, where the overall surface process can be summarized by the following reaction [51]:

$$2Sb(s) + H_2O \rightleftharpoons Sb_2O_3(s) + 6H^+(aq) + 6e^- \quad (1)$$

$$E_r = E^0 - 0.059\ pH\ V; \qquad E_r = -0.1073\ V\ (SCE)$$

The single cathodic peak observed in cyclic voltammograms represents the reduction of the final oxidation product Sb_2O_3 directly to Sb metal according to Eq. (1).

3.3 Cyclic voltammetry on antimony–lead alloy

Fig. 3 represents the cyclic voltammograms obtained on Pb–Sb alloy with 2.7% Sb in 5 M and 0.05 M H_2SO_4 solutions, respectively. In a 5 M H_2SO_4 solution a well-defined anodic peak A′ at 0.1 V and cathodic peak C′ at −0.2 V associated with the oxidation and the reduction of the respective Sb compounds can be seen. Comparing this voltammogram with the one obtained on the pure-Pb electrode (Fig. 1), it can be noticed that the Sb oxidation starts to occur at the potential values at which PbO formation takes place under $PbSO_4$ perm-selective membrane, and the properties of $PbSO_4$ perm-selective membrane influences a great deal the current potential profile in this potential range [52]. The height of both peaks increases with the increasing Sb content. However, on the expanded current scale,

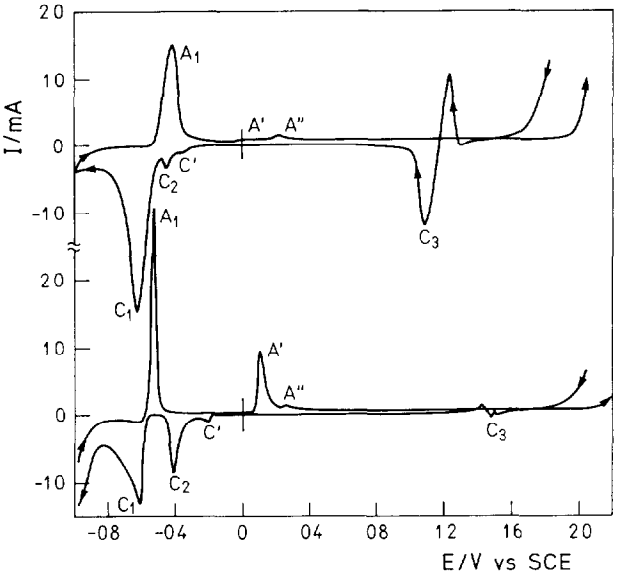

Fig 3. Cyclic voltammograms on a Pb–2.7wt %Sb electrode in a 0 05 M (upper curve) and 5 M (lower curve) H_2SO_4 solution; sweep rate 10 mV s^{-1}

three anodic peaks were observed in the positive going sweep and two cathodic peaks in the negative going sweep, even in the case of the Pb–Sb alloy with the Sb content of 1.3% [52,53]. The other current peaks in Fig. 3 correspond to the oxidation and reduction processes taking place on the pure-Pb electrode.

By comparing the voltammograms of pure Pb with the ones of Pb–Sb alloys, it can be observed that: (i) the current increase due to oxygen evolution and PbO_2 formation on Pb–Sb alloys occurs always at higher potentials rather than on the pure-Pb electrode, and (ii) the anodic current, in the potential range of passive state, is greater on Pb–Sb electrodes than on Pb ones. From the first observation it can be concluded that the oxygen overvoltage on Pb–Sb alloys is higher than on the pure-Pb electrode, as was noticed by Sharpe [7,8], Mahato [12] and Ijomah [41]. On the contrary, Ruetschi and Cahnan [33] and Rogatchev et al. [39] reported that the oxygen overvoltage decreases with the increase of Sb concentration in the Pb–Sb alloy. The second observation can be explained by a larger porosity of the $PbSO_4$ layer on the alloy surface than on the surface of pure Pb. Higher porosity of the $PbSO_4$ formed on Pb–Sb alloys rather than on pure Pb was noticed by many authors [8,31,35,41,42], and was confirmed by the examination of a microstructure of the Pb–Sb alloys and morphology of the $PbSO_4$ crystals [32,34,36], as well as by the impedance measurements [37]. A higher $PbSO_4$ porosity means that the $PbSO_4$ layer becomes less perm-selective, preventing the pH rises to the same extent as on a pure-Pb electrode. This may be the reason why during the anodic oxidation of the alloy electrode, the amount of PbO was found to be less than on a pure-Pb electrode [16]. As a consequence,

cathodic peak C_2 decreases when the Sb content of the alloy increases.

Fig. 3 shows the effect of acid concentration on the cyclic voltammogram of Pb–Sb electrode. The apparent shift of the $PbO_2/PbSO_4$ potential is associated with the acid concentration. The oxygen overpotential is also increased with the increase of acid concentration. It can be seen that there is a rather strong influence of the acid concentration on current peak C_3 and the anodic activity taking place prior to or after the peak C_3. This is a result of the ease of Pb passivation and slower kinetics of $PbSO_4$ to PbO_2 conversion with the increase of acid concentration.

The increased cathodic peak C_2, observed at higher concentration of sulfuric acid, is the reflection of a greater anodic oxidation of the Pb substrate as a tetra-PbO underneath the $PbSO_4$ film. The non-permeability of SO_4^{2-} and HSO_4^- ions in the $PbSO_4$ film apparently increases with the increase of acid concentration, resulting in a greater amount of tetra-PbO as the anodic product in a more concentrated sulfuric acid solution.

The voltammograms in Fig. 3 show that the area of the anodic peak assigned to Sb oxidation is greater than that of the corresponding cathodic peak. This is due to the formation of soluble Sb complexes or ions which, passing through the pores of the $PbSO_4$ layer, leave the electrode. This can be proved by the cathodic peak height dependence on the ratio between the rates of the negative and positive sweeps.

Fig. 4 presents two voltammograms with decreasing ν_a/ν_c ratio at a constant $\nu_a = 1$ mV s^{-1}. It can be seen that the cathodic peak height C′ appears on the voltammogram obtained with the higher negative sweep rate. Under these conditions it can be assumed, that at the upper potential limit, the state of the electrode is one and the same for both voltammograms. At a low cathodic sweep rate ($\nu_c = 2$ mV s^{-1} for the voltammogram in detail of Fig. 4), the Sb(III) species have enough time to leave the pores without being reduced At the high negative sweep rates, they are still in the pores when the potential reaches the range of thermodynamic stability of Sb and a current peak C′ is observed ($\nu_c = 20$ mV s^{-1} for the voltammogram in Fig. 4). Similar behaviour of Sb species during the anodic oxidation of Pb–12wt.%Sb alloy in a 0.5 M H_2SO_4 solution was observed by Pavlov and Monahov [34].

3.4. Electrochemical impedance spectroscopy data

The impedance measurements were performed at potentials where an oxide passive layer is produced anodically on Pb and Pb–Sb alloys under the perm-selective $PbSO_4$ membrane. At the same potential value, the impedance measurements were also performed on the antimony electrode in 0.5 M H_2SO_4 saturated with

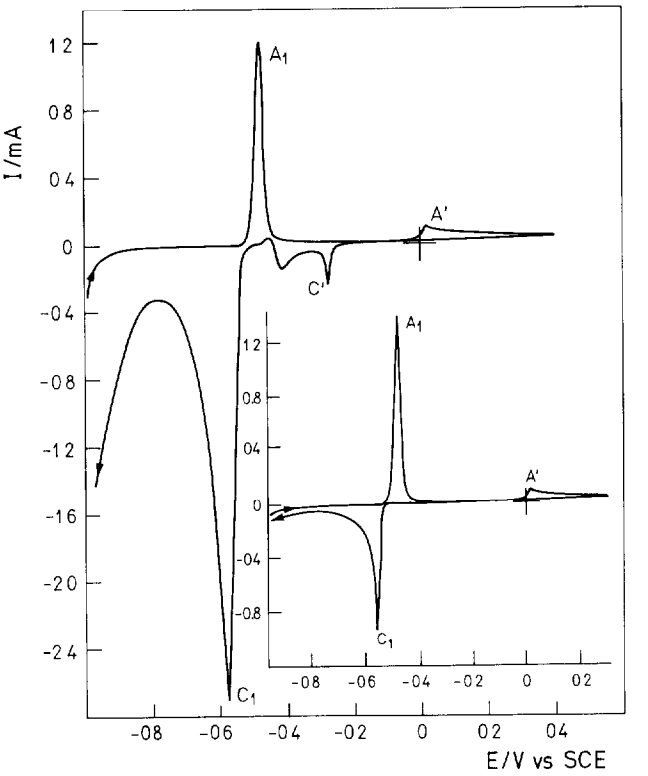

Fig. 4 Cyclic voltammograms on a Pb–4.5wt %Sb electrode in a 0.5 M H_2SO_4 solution. Anodic sweep rate 1 mV s^{-1}, cathodic sweep rate 2 mV s^{-1}, and 20 mV s^{-1} for a voltammogram in detail

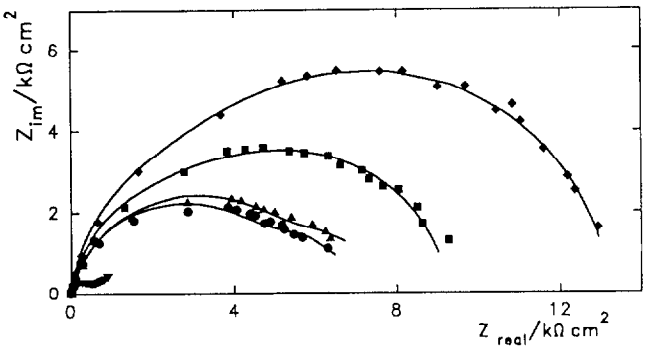

Fig. 5. Nyquist plots for (▼) Sb, (♦) Pb, and Pb-Sb alloys (■) 1.3 wt.%, (▲) 2.7 wt.% and (●) 3.7 wt % in a 0.5 M H_2SO_4 solution.

Sb_2O_3. The results obtained are presented in the Nyquist and Bode plots in Figs. 5 and 6. The impedance diagrams obtained exhibit a capacitive contribution and the capacitative loop diminishes with the increase of the Sb content in the alloy. The impedance spectrum obtained on Sb shows the characteristic charge-transfer resistance semicircle, albeit limited by diffusion. The shape of capacitative loops, thus obtained, indicates that two time constants exist in the impedance spectra of pure Pb and Pb–Sb alloys, as well as on the Sb electrode. This was the reason why the impedance spectra were fitted using the equivalent circuits, shown in Fig. 7. The values of the equivalent circuit elements obtained are listed in Table 1.

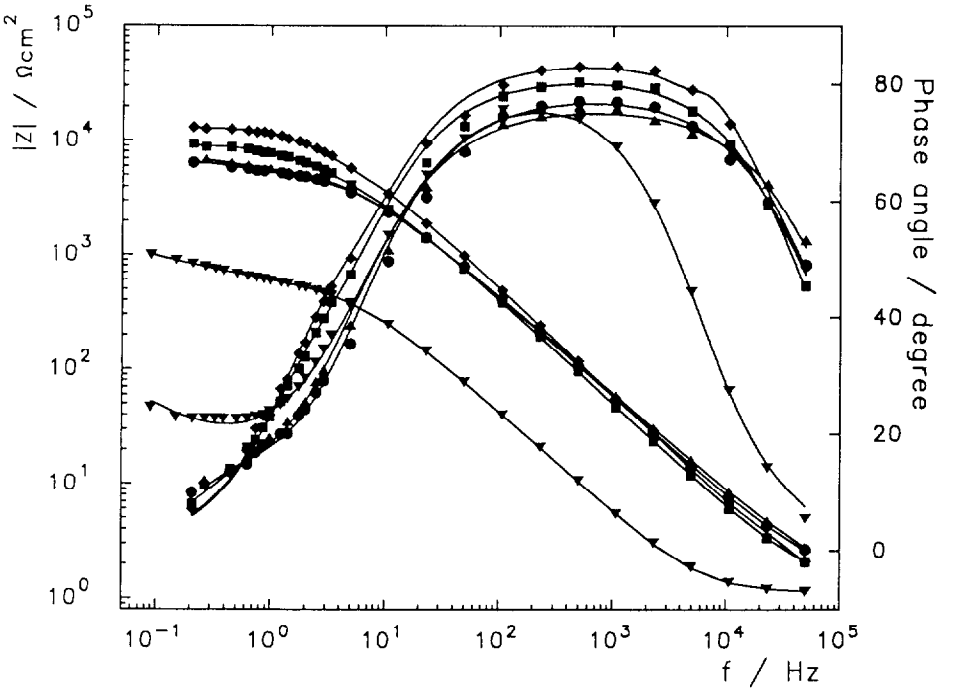

Fig. 6 Bode plots for Sb and Pb–Sb alloys as in Fig 5

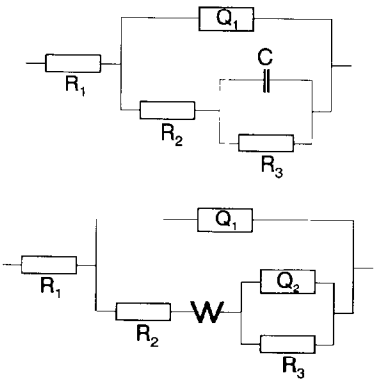

Fig. 7. Equivalent circuits proposed for Sb and Pb–Sb alloy in a 0 5 M H_2SO_4 solution.

More than one time constant has been noticed on both, Sb [54] and Pb electrode [55] in sulfuric acid solution. Based on the results obtained by the cyclic voltammetry and impedance measurements, Bojinov and Pavlov [54] have proposed a two-layer structure of the oxide film on antimony, which was formed by anodic oxidation in 0.5 M H_2SO_4 solution.

Investigating a pure-Pb electrode in a 0.5 M H_2SO_4 solution in a potential range in which a composite $PbSO_4$ + oxide passive layer is produced anodically, Varela et al. [55] have found that the system exhibited a capacitative contribution with two time constants. They have shown that the time constant at higher frequencies diminishes gradually with the decrease of the electrode potential and almost disappears at potentials where the passive layer consists of a single species $PbSO_4$, and, accordingly, it was attributed to the oxide passive layer. Consequently, the capacitive loop at relatively low frequencies was associated with the outer $PbSO_4$ layer.

Accordingly, the resistance and capacitance values presented in Table 1 can be correlated with the outer $PbSO_4$ layer and inner oxide layer in the case of Pb

Table 1
Fit parameters for the experiments in Figs 5 and 6 using the equivalent circuits in Fig. 7

Electrode	R_1 (Ω cm^2)	Q_1 (Ω^{-1} cm^{-2} $s^n \times 10^6$)	n	R_2 (kΩ cm^2)	R_3 (kΩ cm^2)	C (μF cm^{-2})	Q_2 (Ω^{-1} cm^{-2} $s^n \times 10^6$)	n	W^{-1} (Ω^{-1} cm^{-2} $s^{-0.5} \times 10^3$)
Pb	1 00	4 60	0.94	8 47	4 73	11 00			
Pb–1 3wt %Sb	1.01	5 60	0 91	8 15	4 36	18.20			
Pb–2 7wt %Sb	0 99	7.10	0 91	6 73	2.53	30.00			
Pb–3 7wt.%Sb	1.17	9.40	0.85	6.11	1.41	285 00			
Pb–4 5wt.%Sb	0.92	8.30	0 87	5.43	1 45	219 00			
Sb	1.00	52.0	0.93	0.04	0.50		75 00	0.62	2 30

and Pb–Sb alloys and two oxide layers in the case of pure antimony. The inner oxide layer on the antimony electrode shows a higher resistance than the outer one. The similar observation was noticed by Bojinov and Pavlov [54], although the resistance values in this research are somewhat lower, probably due to different electrode pretreatments.

Alloying with Sb causes the decrease in resistance in both sulfate and oxide layer on Pb–Sb alloys, and with the increase of the Sb content the layer resistance decreases.

This observation is in accordance with the cyclic voltammetry results, and confirms the results presented in the literature [8,31,35,41,42].

4. Conclusions

The electrochemical behaviour of Pb, Sb and Pb–Sb binary alloys has been studied as a function of the concentration of sulfuric acid and Sb in the Pb alloy. The investigation was performed by means of cyclic voltammetry and impedance spectroscopy methods.

Cyclic voltammetry, performed between the hydrogen and oxygen evolution and over narrower regions of potential coupled with systematic variation of the scan rates and the positive or negative reversal potential, has revealed more details on the oxidation and reduction processes in the potential region of Pb(II)-, Pb(IV)- and Sb(III)-containing species which give further insight into the nature of the reactions of the lead/acid battery.

The current increase due to PbO_2 formation and oxygen evolution on Pb–Sb alloys always occurred at higher potentials than on pure-Pb electrode indicating that, in spite of high and unknown surface roughness in this potential range, the oxygen overpotential on Pb–Sb alloys is higher than on a pure-Pb electrode.

In the potential range of the passive state, the anodic current was found to be greater on the Pb–Sb electrodes than on Pb one explained by a larger film porosity on the alloy surface. The impedance measurements performed in the potential range of lead oxide, in which Sb oxidation in the alloys takes place, shows a decrease in film resistance caused by increasing Sb content.

References

[1] D. Pavlov, *Electrochim Acta, 23* (1978) 845.
[2] D. Pavlov, *J Electroanal Chem, 118* (1981) 167.
[3] D. Pavlov and Z. Dinev, *J Electrochem. Soc, 127* (1975) 845
[4] D Pavlov, *J Electrochem Soc., 139* (1992) 3075.
[5] H S. Pensar, in D H. Collins (ed.), *Power Sources 3,* Oriel Press, Newcastle-upon-Tyne, 1971, p 79.
[6] G. Archdale and J.A Harrison, *J Electroanal Chem, 34* (1972) 21
[7] T F. Sharpe, *J. Electrochem Soc, 122* (1975) 845
[8] T.F Sharpe, *J. Electrochem Soc, 124* (1977) 168.
[9] J.G. Sunderland, *J Electroanal. Chem., 71* (1976) 341.
[10] P. Casson, N A. Hampson and K. Peters, *J Electrochem Soc, 124* (1977) 1655.
[11] J.C Chang, M.M. Wright and E M.L Valerite, in D H. Collins (ed.), *Power Sources 6,* Academic Press, New York, 1977, p 69.
[12] B K. Mahato, *J Electrochem Soc, 126* (1979) 365.
[13] R.G Barradas and D S Nadezhdin, *Can J Chem, 62* (1984) 596.
[14] V Danile and V. Plichon, *Electrochim Acta, 28* (1983) 781.
[15] S. Flechter and D.B. Matthews, *J Electroanal Chem, 126* (1981) 131.
[16] J.S Buchanan and L.M. Peter, *Electrochim Acta, 33* (1988) 127.
[17] L.J Li, M Fleischmann and L.M Peter, *Electrochim. Acta, 34* (1989) 459
[18] T Laitinen, B Monahov, K. Salmi and G. Sundholm, *Electrochim Acta, 36* (1991) 953.
[19] Y Yamamoto, K. Fumino, T Ueda and M. Nambu, *Electrochim Acta, 37* (1992) 199.
[20] Y Guo, *J Electrochem Soc., 138* (1991) 1222.
[21] Y Guo, *Electrochim Acta, 37* (1992) 495
[22] Y Guo, *J Electrochem Soc., 139* (1992) L99.
[23] D. Pavlov, M Bojinov, T. Laihonen and G. Sundholm, *Electrochim Acta, 36* (1991) 2081.
[24] D Pavlov, M. Bojinov, T. Laitinen and G. Sundholm, *Electrochim Acta, 36* (1991) 2087.
[25] T Laitinen, H. Revitzer, G. Sundholm, J Vilhunen, D. Pavlov and M Bojinov, *Electrochim Acta, 36* (1991) 2093.
[26] I A. Ammar and A. Saad, *J Electranal. Chem., 30* (1971) 395.
[27] M Metikos-Hukovic and B. Lovrecek, *Electrochim Acta, 23* (1980) 717.
[28] M Metikos-Hukovic and B. Lovrecek, *Electrochim Acta, 23* (1978) 1371.
[29] J.L. Dawson, J. Wilkinson and M.I Gillibrand, *J Inorg Nucl Chem, 32* (1970) 501.
[30] S. Laihonen, T Laitinen, G Sundholm and A Yli-Pentti, *Electrochim Acta, 35* (1990) 229
[31] P Ruetschi, *J Electrochem Soc, 120* (1973) 331.
[32] D. Pavlov and B Monahov, *J Electroanal Chem, 305* (1991) 57.
[33] P Ruetschi and B.D Cahan, *J Electrochem. Soc, 105* (1958) 369
[34] D. Pavlov and B Monahov, *J Electroanal Chem, 218* (1987) 135
[35] N A Hampson, S. Kelly and K. Peters, *J Appl. Electrochem, 10* (1980) 91
[36] A.G. Gaad Allah, H A.A. El-Rahman, S.A Salih and M A El-Galil, *J Appl. Electrochem, 22* (1992) 571
[37] M.P.J. Brennan, B.N Stirrup and N A Hampson, *J Appl Electrochem., 4* (1974) 497.
[38] J.A Bialacki, N.A Hampson and F. Wilson, *J Appl Electrochem, 15* (1985) 99
[39] T. Rogatchev, St Ruevski and D. Pavlov, *J Appl. Electrochem, 6* (1976) 33.
[40] T. Laitinen, K Salmi, S. Sundholm, B. Monahov and D. Pavlov, *Electrochim. Acta, 36* (1991) 605.
[41] M.N Ijomah, *J Electrochem Soc., 134* (1987) 1960
[42] S. Webster, P J Mitchell, N A Hampson and D.I. Dyson, *J Electrochem. Soc, 133* (1986) 137
[43] V. Danile and V Plichon, *Electrochim Acta, 28* (1983) 785, and refs. therein
[44] D Pavlov, *Electrochim Acta, 13* (1968) 2051.
[45] D Pavlov and R. Popova, *Electrochim. Acta, 15* (1970) 1483
[46] D Pavlov, S. Zanova and G Papazov, *J. Electrochem Soc, 124* (1977) 1522.

[47] M. Fleischmann and H.R Thirsk, *Trans Faraday Soc*, *51* (1955) 71.

[48] J.P. Carr, N.A Hampson and R. Taylor, *J Electroanal Chem*, *33* (1971) 109.

[49] D. Pavlov and N Iordanov, *J Electrochem Soc*, *117* (1970) 1103.

[50] E.M L Valeriote and L.D. Gallop, *J Electrochem Soc*, *124* (1977) 370.

[51] M. Pourbaix, *Atlas of Electrochemical Equilibria in Aqueous Solutions*, Pergamon, Oxford, 1966, p 524

[52] M Metikos-Hukovic, R Babic and S. Omanovic, *J Electroanal Chem*, in press.

[53] R. Babic, M. Metikos-Hukovic, S. Brinic and Z. Grubac, *Proc Int. Conf Lead/Acid Batteries, LABAT '93, St Konstantin, Varna, Bulgaria, June 7–11 1993*, p. 57; *The Battery Man, 35* (1993) 20.

[54] M. Bojinov and D. Pavlov, *J. Electroanal. Chem*, *315* (1991) 301.

[55] F.E. Varela, L M. Gassa and J.R Vilche, *J. Electroanal Chem*, *353* (1993) 147.